Wavelets on the sphere and cosmological applications

Jason McEwen
http://www.jasonmcewen.org/

LTS2, Institute of Electrical Engineering,
Ecole Polytechnique Fédérale de Lausanne (EPFL), Switzerland

Guest Lecture for Advanced Signal Processing :: November 2010

Outline

Outline

Cosmological concordance model

- Concordance model of modern cosmology emerged recently with many cosmological parameters constrained to high precision.
- General description is of a Universe undergoing accelerated expansion, containing 4% ordinary baryonic matter, 22% cold dark matter and 74% dark energy.
- Structure and evolution of the Universe constrained through cosmological observations.

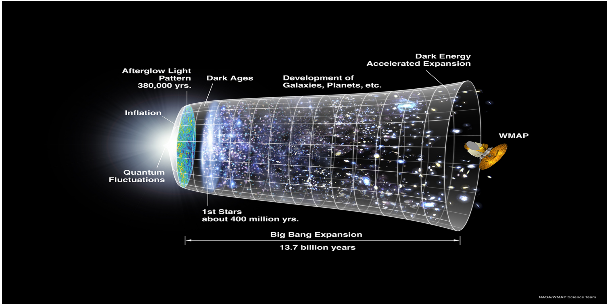

Credit: WMAP Science Team

Cosmic microwave background (CMB)

- Temperature of early Universe sufficiently hot that photons had enough energy to ionise hydrogen.
- Compton scattering happened frequently $\Rightarrow$ mean free path of photons extremely small.
- Universe consisted of an opaque photon-baryon fluid.
- As Universe expanded it cooled, until majority of photons no longer had sufficient energy to ionise hydrogen.
- Photons decoupled from baryons and the Universe became essentially transparent to radiation.
- *Recombination* occurred when temperature of Universe dropped to 3000K ($\sim$400,000 years after the Big Bang).
- Photons then free to propagate largely unhindered and observed today on celestial sphere as CMB radiation.
- CMB is highly uniform over the celestial sphere, however it contains small fluctuations at a relative level of 10^{-5} due to acoustic oscillations in the early Universe.
- CMB observed on spherical manifold, hence the geometry of the sphere must be taken into account in any analysis.

Cosmic microwave background (CMB)

- Temperature of early Universe sufficiently hot that photons had enough energy to ionise hydrogen.
- Compton scattering happened frequently $\Rightarrow$ mean free path of photons extremely small.
- Universe consisted of an opaque photon-baryon fluid.
- As Universe expanded it cooled, until majority of photons no longer had sufficient energy to ionise hydrogen.
- Photons decoupled from baryons and the Universe became essentially transparent to radiation.
- *Recombination* occurred when temperature of Universe dropped to 3000K ($\sim$400,000 years after the Big Bang).
- Photons then free to propagate largely unhindered and observed today on celestial sphere as CMB radiation.
- CMB is highly uniform over the celestial sphere, however it contains small fluctuations at a relative level of 10^{-5} due to acoustic oscillations in the early Universe.
- CMB observed on spherical manifold, hence the geometry of the sphere must be taken into account in any analysis.

Cosmic microwave background (CMB)

- Temperature of early Universe sufficiently hot that photons had enough energy to ionise hydrogen.
- Compton scattering happened frequently $\Rightarrow$ mean free path of photons extremely small.
- Universe consisted of an opaque photon-baryon fluid.
- As Universe expanded it cooled, until majority of photons no longer had sufficient energy to ionise hydrogen.
- Photons decoupled from baryons and the Universe became essentially transparent to radiation.
- *Recombination* occurred when temperature of Universe dropped to 3000K ($\sim$400,000 years after the Big Bang).

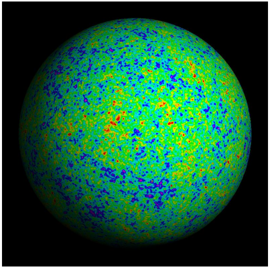

Credit: Max Tegmark

- Photons then free to propagate largely unhindered and observed today on celestial sphere as CMB radiation.
- CMB is highly uniform over the celestial sphere, however it contains small fluctuations at a relative level of 10^{-5} due to acoustic oscillations in the early Universe.
- CMB observed on spherical manifold, hence the geometry of the sphere must be taken into account in any analysis.

Cosmic microwave background (CMB)

- Quantum fluctuations in the early Universe blown to macroscopic scales by inflation, establishing acoustic oscillations in primordial plasma of the very early Universe.
- Provide the seeds of structure formation in our Universe.
- Cosmological concordance model explains the power spectrum of these oscillations to very high precision.
- Although a general cosmological concordance model is now established, many details remain unclear. Study of more exotic cosmological models now important.

Cosmic microwave background (CMB)

- Quantum fluctuations in the early Universe blown to macroscopic scales by inflation, establishing acoustic oscillations in primordial plasma of the very early Universe.
- Provide the seeds of structure formation in our Universe.
- Cosmological concordance model explains the power spectrum of these oscillations to very high precision.

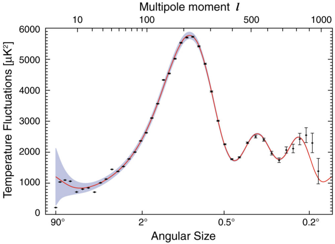

Credit: WMAP Science Team

- Although a general cosmological concordance model is now established, many details remain unclear. Study of more exotic cosmological models now important.

Cosmic microwave background (CMB)

- Quantum fluctuations in the early Universe blown to macroscopic scales by inflation, establishing acoustic oscillations in primordial plasma of the very early Universe.
- Provide the seeds of structure formation in our Universe.
- Cosmological concordance model explains the power spectrum of these oscillations to very high precision.

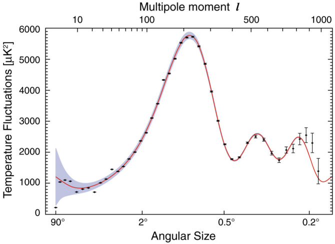

Credit: WMAP Science Team

- Although a general cosmological concordance model is now established, many details remain unclear. Study of more exotic cosmological models now important.

Observations of the CMB

- Full-sky observations of the CMB ongoing.

(a) COBE (launched 1989)

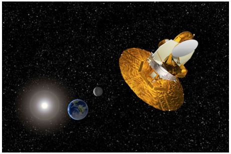

(b) WMAP (launched 2001)

(c) Planck (launched 2009)

Figure: Full-sky CMB observations

- Each new experiment provides dramatic improvement in precision and resolution of observations (*e.g.* COBE to WMAP illustration).

Observations of the CMB

- Full-sky observations of the CMB ongoing.

(a) COBE (launched 1989)

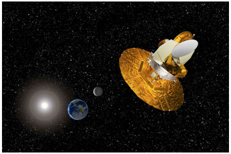

(b) WMAP (launched 2001)

(c) Planck (launched 2009)

Figure: Full-sky CMB observations

- Each new experiment provides dramatic improvement in precision and resolution of observations (*e.g.* COBE to WMAP illustration).

(cobe 2 wmap movie)

Credit: WMAP Science Team

Outline

Recall wavelet transform in Euclidean space

- Project signal onto wavelets

$$\mathcal{W}^f(a,b) = \langle f, \psi_{a,b} \rangle = |a|^{-1/2} \int_{-\infty}^{\infty} \mathrm{d}t\, f(t)\, \psi^* \left(\frac{t-b}{a} \right),$$

where $\psi_{a,b} = |a|^{-1/2} \psi(\frac{t-b}{a})$.

- Synthesis signal from wavelet coefficients

$$f(t) = C_\psi^{-1} \int_{-\infty}^{\infty} \mathrm{d}b \int_0^{\infty} \frac{\mathrm{d}a}{a^2}\, \mathcal{W}^f(a,b) \psi_{a,b}(t).$$

- Admissibility condition to ensure perfect reconstruction

$$0 < C_\psi \equiv \int_{-\infty}^{\infty} \frac{\mathrm{d}k}{|k|}\, |\hat{\psi}(k)|^2 < \infty.$$

- Construct on sphere in analogous manner.

Wavelets on the sphere

- Follow construction derived by Antoine and Vandergheynst (1998) [1] (reintroduced by Wiaux (2005) [8]).
- Construct wavelet atoms from affine transformations (dilation, translation) on the sphere of a mother wavelet.
- The natural extension of translations to the sphere are rotations. Characterised by the elements of the rotation group $\mathrm{SO}(3)$, which parameterise in terms of the three Euler angles $\rho = (\alpha, \beta, \gamma)$. Rotation of a function f on the sphere is defined by

$$[\mathcal{R}(\rho)f](\omega) = f(\rho^{-1}\omega), \quad \rho \in \mathrm{SO}(3) .$$

- How define dilation and admissible wavelets on the sphere?

Wavelets on the sphere

- Follow construction derived by Antoine and Vandergheynst (1998) [1] (reintroduced by Wiaux (2005) [8]).
- Construct wavelet atoms from affine transformations (dilation, translation) on the sphere of a mother wavelet.
- The natural extension of translations to the sphere are rotations. Characterised by the elements of the rotation group $\mathrm{SO}(3)$, which parameterise in terms of the three Euler angles $\rho = (\alpha, \beta, \gamma)$. Rotation of a function f on the sphere is defined by

$$[\mathcal{R}(\rho)f](\omega) = f(\rho^{-1}\omega), \quad \rho \in \mathrm{SO}(3) \ .$$

- How define dilation and admissible wavelets on the sphere?

Wavelets on the sphere

- Follow construction derived by Antoine and Vandergheynst (1998) [1] (reintroduced by Wiaux (2005) [8]).
- Construct wavelet atoms from affine transformations (dilation, translation) on the sphere of a mother wavelet.
- The natural extension of translations to the sphere are rotations. Characterised by the elements of the rotation group $\mathrm{SO}(3)$, which parameterise in terms of the three Euler angles $\rho = (\alpha, \beta, \gamma)$. Rotation of a function f on the sphere is defined by

$$[\mathcal{R}(\rho)f](\omega) = f(\rho^{-1}\omega), \quad \rho \in \mathrm{SO}(3) \ .$$

- How define dilation and admissible wavelets on the sphere?

Stereographic projection

- Apply stereographic projection to build an association with the plane.

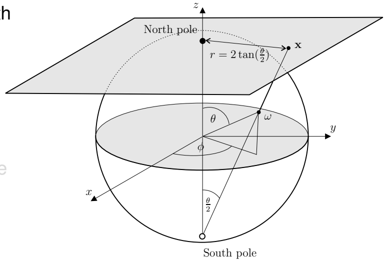

- Stereographic projection operator is defined by $\Pi : \omega \rightarrow \boldsymbol{x} = \Pi\omega = (r(\theta), \phi)$ where $r = 2\tan(\theta/2)$, $\omega \equiv (\theta, \phi) \in \mathbb{S}^2$ and $\boldsymbol{x} \in \mathbb{R}^2$ is a point in the plane, denoted here by the polar coordinates (r, ϕ). The inverse operator is $\Pi^{-1} : \boldsymbol{x} \rightarrow \omega = \Pi^{-1}\boldsymbol{x} = (\theta(r), \phi)$, where $\theta(r) = 2\tan^{-1}(r/2)$.

- Define the action of the stereographic projection operator on functions on the plane and sphere. Consider the space of square integrable functions in $\mathrm{L}^2(\mathbb{R}^2, \mathrm{d}^2\boldsymbol{x})$ on the plane and $\mathrm{L}^2(\mathbb{S}^2, \mathrm{d}\Omega(\omega))$ on the sphere.
  - The action of the stereographic projection operator $\Pi : f \in \mathrm{L}^2(\mathbb{S}^2, \mathrm{d}\Omega(\omega)) \rightarrow p = \Pi f \in \mathrm{L}^2(\mathbb{R}^2, \mathrm{d}^2\boldsymbol{x})$ on functions is defined as
$$p(r, \phi) = (\Pi f)(r, \phi) = (1 + r^2/4)^{-1} f(\theta(r), \phi) \; .$$
  - The inverse stereographic projection operator $\Pi^{-1} : p \in \mathrm{L}^2(\mathbb{R}^2, \mathrm{d}^2\boldsymbol{x}) \rightarrow f = \Pi^{-1} p \in \mathrm{L}^2(\mathbb{S}^2, \mathrm{d}\Omega(\omega))$ on functions is then
$$f(\theta, \phi) = (\Pi^{-1} p)(\theta, \phi) = [1 + \tan^2(\theta/2)] p(r(\theta), \phi) \; .$$

Stereographic projection

- Apply stereographic projection to build an association with the plane.

- Stereographic projection operator is defined by $\Pi : \omega \rightarrow \boldsymbol{x} = \Pi\omega = (r(\theta), \phi)$ where $r = 2\tan(\theta/2)$, $\omega \equiv (\theta, \phi) \in \mathbb{S}^2$ and $\boldsymbol{x} \in \mathbb{R}^2$ is a point in the plane, denoted here by the polar coordinates (r, ϕ). The inverse operator is $\Pi^{-1} : \boldsymbol{x} \rightarrow \omega = \Pi^{-1}\boldsymbol{x} = (\theta(r), \phi)$, where $\theta(r) = 2\tan^{-1}(r/2)$.

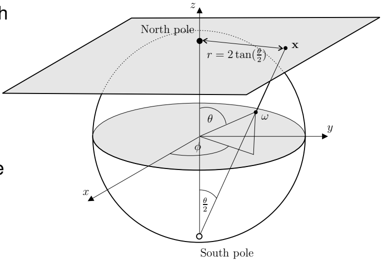

- Define the action of the stereographic projection operator on functions on the plane and sphere. Consider the space of square integrable functions in $\mathrm{L}^2(\mathbb{R}^2, \mathrm{d}^2\boldsymbol{x})$ on the plane and $\mathrm{L}^2(\mathbb{S}^2, \mathrm{d}\Omega(\omega))$ on the sphere.
  - The action of the stereographic projection operator $\Pi : f \in \mathrm{L}^2(\mathbb{S}^2, \mathrm{d}\Omega(\omega)) \rightarrow p = \Pi f \in \mathrm{L}^2(\mathbb{R}^2, \mathrm{d}^2\boldsymbol{x})$ on functions is defined as

$$p(r, \phi) = (\Pi f)(r, \phi) = (1 + r^2/4)^{-1} f(\theta(r), \phi) .$$

  - The inverse stereographic projection operator $\Pi^{-1} : p \in \mathrm{L}^2(\mathbb{R}^2, \mathrm{d}^2\boldsymbol{x}) \rightarrow f = \Pi^{-1} p \in \mathrm{L}^2(\mathbb{S}^2, \mathrm{d}\Omega(\omega))$ on functions is then

$$f(\theta, \phi) = (\Pi^{-1} p)(\theta, \phi) = [1 + \tan^2(\theta/2)] p(r(\theta), \phi) .$$

Stereographic projection

- Apply stereographic projection to build an association with the plane.

- Stereographic projection operator is defined by $\Pi : \omega \rightarrow \boldsymbol{x} = \Pi\omega = (r(\theta), \phi)$ where $r = 2\tan(\theta/2)$, $\omega \equiv (\theta, \phi) \in \mathbb{S}^2$ and $\boldsymbol{x} \in \mathbb{R}^2$ is a point in the plane, denoted here by the polar coordinates (r, ϕ). The inverse operator is $\Pi^{-1} : \boldsymbol{x} \rightarrow \omega = \Pi^{-1}\boldsymbol{x} = (\theta(r), \phi)$, where $\theta(r) = 2\tan^{-1}(r/2)$.

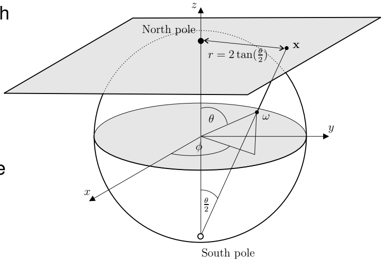

- Define the action of the stereographic projection operator on functions on the plane and sphere. Consider the space of square integrable functions in $\mathrm{L}^2(\mathbb{R}^2,\, \mathrm{d}^2\boldsymbol{x})$ on the plane and $\mathrm{L}^2(\mathbb{S}^2,\, \mathrm{d}\Omega(\omega))$ on the sphere.
  - The action of the stereographic projection operator $\Pi : f \in \mathrm{L}^2(\mathbb{S}^2,\, \mathrm{d}\Omega(\omega)) \rightarrow p = \Pi f \in \mathrm{L}^2(\mathbb{R}^2,\, \mathrm{d}^2\boldsymbol{x})$ on functions is defined as

$$p(r, \phi) = (\Pi f)(r, \phi) = (1 + r^2/4)^{-1} f(\theta(r), \phi) \; .$$

  - The inverse stereographic projection operator $\Pi^{-1} : p \in \mathrm{L}^2(\mathbb{R}^2,\, \mathrm{d}^2\boldsymbol{x}) \rightarrow f = \Pi^{-1}p \in \mathrm{L}^2(\mathbb{S}^2,\, \mathrm{d}\Omega(\omega))$ on functions is then

$$f(\theta, \phi) = (\Pi^{-1}p)(\theta, \phi) = [1 + \tan^2(\theta/2)]p(r(\theta), \phi) \; .$$

Dilation on the sphere

- The spherical dilation operator $\mathcal{D}(a) : f(\omega) \rightarrow [\mathcal{D}(a)f](\omega)$ in $\mathrm{L}^2(\mathbb{S}^2, \, \mathrm{d}\Omega(\omega))$ is defined as the conjugation by Π of the Euclidean dilation $d(a)$ in $\mathrm{L}^2(\mathbb{R}^2, \, \mathrm{d}^2\boldsymbol{x})$ on tangent plane at north pole:

$$\mathcal{D}(a) \equiv \Pi^{-1} \, d(a) \, \Pi \, .$$

- Spherical dilation given by

$$[\mathcal{D}(a)f](\omega) = [\lambda(a, \theta, \phi)]^{1/2} \, f(\omega_{1/a}) \, ,$$

where $\omega_a = (\theta_a, \phi)$ and $\tan(\theta_a/2) = a \tan(\theta/2)$.

- Cocycle of a spherical dilation is defined by

$$\lambda(a, \theta, \phi) \equiv \frac{4a^2}{[(a^2 - 1)\cos\theta + (a^2 + 1)]^2} \, .$$

Wavelet analysis formula

- Wavelets on the sphere may now be constructed from rotations and dilations of a mother spherical wavelet $\psi \in \mathrm{L}^2(\mathbb{S}^2,\, \mathrm{d}\Omega(\omega))$. The corresponding wavelet family $\{\psi_{a,\rho} \equiv \mathcal{R}(\rho)\mathcal{D}(a)\psi \,:\, \rho \in \mathrm{SO}(3),\, a \in \mathbb{R}_*^+\}$ provides an over-complete set of functions in $\mathrm{L}^2(\mathbb{S}^2,\, \mathrm{d}\Omega(\omega))$.
- The CSWT of $f \in \mathrm{L}^2(\mathbb{S}^2,\, \mathrm{d}\Omega(\omega))$ is given by the projection on to each wavelet atom in the usual manner:

$$\boxed{\mathcal{W}^f(a,\rho) = \langle f, \psi_{a,\rho}\rangle = \int_{\mathbb{S}^2} \mathrm{d}\Omega(\omega)\, f(\omega)\, \psi^*_{a,\rho}(\omega)\ ,}$$

where $\mathrm{d}\Omega(\omega) = \sin\theta \,\mathrm{d}\theta\,\mathrm{d}\phi$ is the usual invariant measure on the sphere.
- Transform general in the sense that all orientations in the rotation group $\mathrm{SO}(3)$ are considered, thus directional structure is naturally incorporated.
- Fast algorithms essential (for a review see [9])
  - Factoring of rotations: JDM *et al.* 2007 [4]
  - Separation of variables: Wiaux *et al.* 2005 [10]

Wavelet analysis formula

- Wavelets on the sphere may now be constructed from rotations and dilations of a mother spherical wavelet $\psi \in \mathrm{L}^2(\mathbb{S}^2, \,\mathrm{d}\Omega(\omega))$. The corresponding wavelet family $\{\psi_{a,\rho} \equiv \mathcal{R}(\rho)\mathcal{D}(a)\psi \,:\, \rho \in \mathrm{SO}(3),\, a \in \mathbb{R}_*^+\}$ provides an over-complete set of functions in $\mathrm{L}^2(\mathbb{S}^2, \,\mathrm{d}\Omega(\omega))$.
- The CSWT of $f \in \mathrm{L}^2(\mathbb{S}^2, \,\mathrm{d}\Omega(\omega))$ is given by the projection on to each wavelet atom in the usual manner:

$$\boxed{\mathcal{W}^f(a,\rho) = \langle f, \psi_{a,\rho} \rangle = \int_{\mathbb{S}^2} \mathrm{d}\Omega(\omega)\, f(\omega)\, \psi_{a,\rho}^*(\omega) \,,}$$

  where $\mathrm{d}\Omega(\omega) = \sin\theta \,\mathrm{d}\theta\,\mathrm{d}\phi$ is the usual invariant measure on the sphere.
- Transform general in the sense that all orientations in the rotation group $\mathrm{SO}(3)$ are considered, thus directional structure is naturally incorporated.
- Fast algorithms essential (for a review see [9])
  - Factoring of rotations: JDM *et al.* 2007 [4]
  - Separation of variables: Wiaux *et al.* 2005 [10]

Wavelet analysis formula

- Wavelets on the sphere may now be constructed from rotations and dilations of a mother spherical wavelet $\psi \in \mathrm{L}^2(\mathbb{S}^2, \mathrm{d}\Omega(\omega))$. The corresponding wavelet family $\{\psi_{a,\rho} \equiv \mathcal{R}(\rho)\mathcal{D}(a)\psi : \rho \in \mathrm{SO}(3), a \in \mathbb{R}_*^+\}$ provides an over-complete set of functions in $\mathrm{L}^2(\mathbb{S}^2, \mathrm{d}\Omega(\omega))$.
- The CSWT of $f \in \mathrm{L}^2(\mathbb{S}^2, \mathrm{d}\Omega(\omega))$ is given by the projection on to each wavelet atom in the usual manner:

$$\boxed{\mathcal{W}^f(a, \rho) = \langle f, \psi_{a,\rho} \rangle = \int_{\mathbb{S}^2} \mathrm{d}\Omega(\omega)\, f(\omega)\, \psi_{a,\rho}^*(\omega)\ ,}$$

  where $\mathrm{d}\Omega(\omega) = \sin\theta\, \mathrm{d}\theta\, \mathrm{d}\phi$ is the usual invariant measure on the sphere.
- Transform general in the sense that all orientations in the rotation group $\mathrm{SO}(3)$ are considered, thus directional structure is naturally incorporated.
- Fast algorithms essential (for a review see [9])
  - Factoring of rotations: JDM *et al.* 2007 [4]
  - Separation of variables: Wiaux *et al.* 2005 [10]

Wavelet synthesis formula

- The synthesis of a signal on the sphere from its wavelet coefficients is given by

$$\boxed{f(\omega) = \int_0^\infty \frac{\mathrm{d}a}{a^3} \int_{\mathrm{SO}(3)} \mathrm{d}\varrho(\rho) \mathcal{W}^f(a, \rho)\, [\mathcal{R}(\rho)\widehat{L}_\psi \psi_a](\omega)\ ,}$$

where $\mathrm{d}\varrho(\rho) = \sin\beta\, \mathrm{d}\alpha\, \mathrm{d}\beta\, \mathrm{d}\gamma$ is the invariant measure on the rotation group $\mathrm{SO}(3)$.

- The $\widehat{L}_\psi$ operator in $\mathrm{L}^2(\mathbb{S}^2,\ \mathrm{d}\Omega(\omega))$ is defined by the action

$$(\widehat{L}_\psi g)_{\ell m} \equiv g_{\ell m} / \widehat{C}_\psi^\ell$$

on the spherical harmonic coefficients of functions $g \in \mathrm{L}^2(\mathbb{S}^2,\ \mathrm{d}\Omega(\omega))$.

- In order to ensure the perfect reconstruction of a signal synthesised from its wavelet coefficients, the admissibility condition

$$\boxed{0 < \widehat{C}_\psi^\ell \equiv \frac{8\pi^2}{2\ell+1} \sum_{m=-\ell}^{\ell} \int_0^\infty \frac{\mathrm{d}a}{a^3} \mid (\psi_a)_{\ell m} \mid^2 < \infty}$$

must be satisfied for all $\ell \in \mathbb{N}$, where $(\psi_a)_{\ell m}$ are the spherical harmonic coefficients of $\psi_a(\omega)$.

Wavelet synthesis formula

- The synthesis of a signal on the sphere from its wavelet coefficients is given by

$$\boxed{f(\omega) = \int_0^\infty \frac{\mathrm{d}a}{a^3} \int_{\mathrm{SO}(3)} \mathrm{d}\varrho(\rho) \mathcal{W}^f(a,\rho)\, [\mathcal{R}(\rho)\widehat{L}_\psi \psi_a](\omega)\ ,}$$

where $\mathrm{d}\varrho(\rho) = \sin\beta \,\mathrm{d}\alpha\, \mathrm{d}\beta\, \mathrm{d}\gamma$ is the invariant measure on the rotation group $\mathrm{SO}(3)$.

- The $\widehat{L}_\psi$ operator in $\mathrm{L}^2(\mathbb{S}^2, \mathrm{d}\Omega(\omega))$ is defined by the action

$$(\widehat{L}_\psi g)_{\ell m} \equiv g_{\ell m} / \widehat{C}_\psi^\ell$$

on the spherical harmonic coefficients of functions $g \in \mathrm{L}^2(\mathbb{S}^2, \mathrm{d}\Omega(\omega))$.

- In order to ensure the perfect reconstruction of a signal synthesised from its wavelet coefficients, the admissibility condition

$$\boxed{0 < \widehat{C}_\psi^\ell \equiv \frac{8\pi^2}{2\ell+1} \sum_{m=-\ell}^{\ell} \int_0^\infty \frac{\mathrm{d}a}{a^3} \mid (\psi_a)_{\ell m} \mid^2 < \infty}$$

must be satisfied for all $\ell \in \mathbb{N}$, where $(\psi_a)_{\ell m}$ are the spherical harmonic coefficients of $\psi_a(\omega)$.

Correspondence principle

- Correspondence principle between spherical and Euclidean wavelets states that the inverse stereographic projection of an *admissible* wavelet on the plane yields an *admissible* wavelet on the sphere (proved by Wiaux *et al.* 2005 [8].)
- Mother wavelets on sphere constructed from the projection of mother Euclidean wavelets defined on the plane:

$$\psi = \Pi^{-1} \psi_{\mathbb{R}^2} \ ,$$

  where $\psi_{\mathbb{R}^2} \in \mathrm{L}^2(\mathbb{R}^2, \, \mathrm{d}^2\boldsymbol{x})$ is an admissible wavelet in the plane.
- Directional wavelets on sphere may be naturally constructed in this setting – they are simply the projection of directional Euclidean planar wavelets on to the sphere.

Correspondence principle

- Correspondence principle between spherical and Euclidean wavelets states that the inverse stereographic projection of an *admissible* wavelet on the plane yields an *admissible* wavelet on the sphere (proved by Wiaux *et al.* 2005 [8].)
- Mother wavelets on sphere constructed from the projection of mother Euclidean wavelets defined on the plane:

$$\psi = \Pi^{-1}\psi_{\mathbb{R}^2} \ ,$$

where $\psi_{\mathbb{R}^2} \in \mathrm{L}^2(\mathbb{R}^2, \, \mathrm{d}^2\boldsymbol{x})$ is an admissible wavelet in the plane.

- Directional wavelets on sphere may be naturally constructed in this setting – they are simply the projection of directional Euclidean planar wavelets on to the sphere.

Correspondence principle

- Correspondence principle between spherical and Euclidean wavelets states that the inverse stereographic projection of an *admissible* wavelet on the plane yields an *admissible* wavelet on the sphere (proved by Wiaux *et al.* 2005 [8].)
- Mother wavelets on sphere constructed from the projection of mother Euclidean wavelets defined on the plane:

$$\psi = \Pi^{-1}\psi_{\mathbb{R}^2} \; ,$$

where $\psi_{\mathbb{R}^2} \in \mathrm{L}^2(\mathbb{R}^2, \, \mathrm{d}^2\boldsymbol{x})$ is an admissible wavelet in the plane.

- Directional wavelets on sphere may be naturally constructed in this setting – they are simply the projection of directional Euclidean planar wavelets on to the sphere.

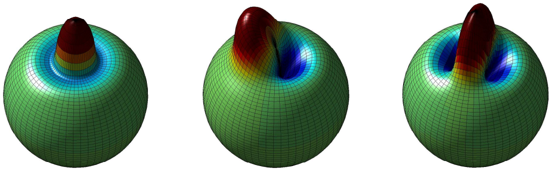

(a) SMHW (b) SBW (c) S2GDW

Figure: Spherical wavelets at scale $a, b = 0.2$.

Gaussianity of the CMB

- Statistics of primordial fluctuations provide a useful mechanism for distinguishing between various scenarios of the early Universe, such as various models of inflation.
- Primordial fluctuations give rise to the CMB anisotropies.
- In the simplest inflationary scenarios, primordial perturbations seed Gaussian temperature fluctuations in the CMB.
- However, this is not the case for non-standard inflationary models.
- Evidence of non-Gaussianity in the CMB anisotropies would therefore have profound implications for the standard cosmological concordance model.
- Probe WMAP observations of the CMB for evidence of non-Gaussianity.

Gaussianity of the CMB

- Statistics of primordial fluctuations provide a useful mechanism for distinguishing between various scenarios of the early Universe, such as various models of inflation.
- Primordial fluctuations give rise to the CMB anisotropies.
- In the simplest inflationary scenarios, primordial perturbations seed Gaussian temperature fluctuations in the CMB.
- However, this is not the case for non-standard inflationary models.
- Evidence of non-Gaussianity in the CMB anisotropies would therefore have profound implications for the standard cosmological concordance model.
- Probe WMAP observations of the CMB for evidence of non-Gaussianity.

Gaussianity of the CMB

- Statistics of primordial fluctuations provide a useful mechanism for distinguishing between various scenarios of the early Universe, such as various models of inflation.
- Primordial fluctuations give rise to the CMB anisotropies.
- In the simplest inflationary scenarios, primordial perturbations seed Gaussian temperature fluctuations in the CMB.
- However, this is not the case for non-standard inflationary models.
- Evidence of non-Gaussianity in the CMB anisotropies would therefore have profound implications for the standard cosmological concordance model.
- Probe WMAP observations of the CMB for evidence of non-Gaussianity.

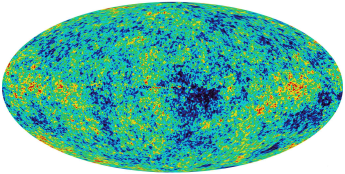

Wavelet analysis of Gaussianity of the CMB

- Various physical processes manifest at different scales and locations, hence employ wavelet analysis to probe CMB.
- Wavelet coefficients of Gaussian signal remain Gaussian distributed (due to linearity of wavelet transform).
- Examine the skewness and kurtosis of wavelet coefficients.
- Compare to Monte Carlo simulations of Gaussian CMB realisations.
- Significant non-Gaussian signal detected in the skewness of wavelet coefficients.

Wavelet analysis of Gaussianity of the CMB

- Various physical processes manifest at different scales and locations, hence employ wavelet analysis to probe CMB.
- Wavelet coefficients of Gaussian signal remain Gaussian distributed (due to linearity of wavelet transform).
- Examine the skewness and kurtosis of wavelet coefficients.
- Compare to Monte Carlo simulations of Gaussian CMB realisations.
- Significant non-Gaussian signal detected in the skewness of wavelet coefficients.

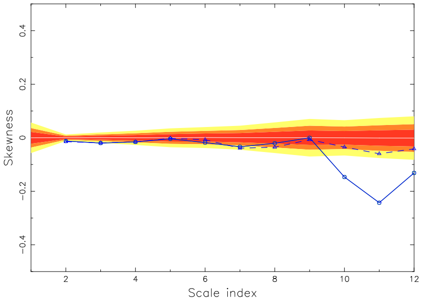

Figure: Skewness of wavelet coefficients

Wavelet analysis of Gaussianity of the CMB

- Various physical processes manifest at different scales and locations, hence employ wavelet analysis to probe CMB.
- Wavelet coefficients of Gaussian signal remain Gaussian distributed (due to linearity of wavelet transform).
- Examine the skewness and kurtosis of wavelet coefficients.
- Compare to Monte Carlo simulations of Gaussian CMB realisations.
- Significant non-Gaussian signal detected in the skewness of wavelet coefficients.

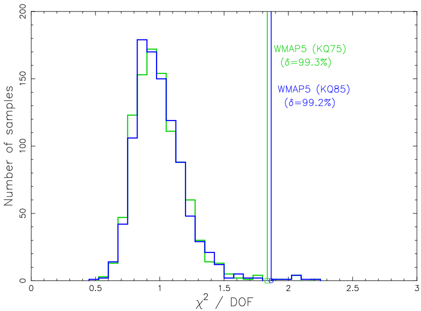

Figure: χ^2 of skewness of wavelet coefficients

Localisation of non-Gaussian features in the CMB

- Localise regions that contribute most significantly to the non-Gaussian signal.
- Detection of the "cold spot" anomaly in the CMB.
- Various new cosmology models constructed in attempt to explain the cold spot.

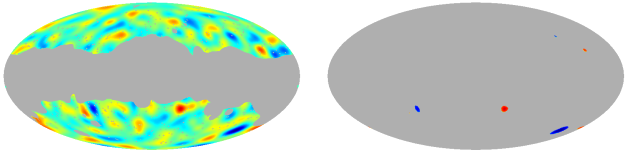

(a) SMHW coefficients

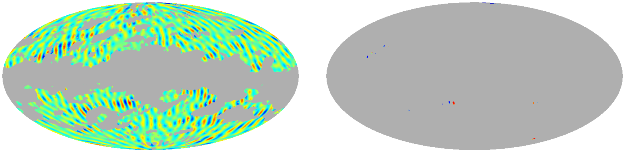

(b) SMW coefficients

Figure: Spherical wavelet coefficient maps (left) and thresholded maps (right)

Localisation of non-Gaussian features in the CMB

- Localise regions that contribute most significantly to the non-Gaussian signal.
- Detection of the "cold spot" anomaly in the CMB.
- Various new cosmology models constructed in attempt to explain the cold spot.

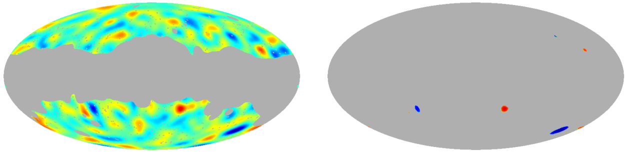

(a) SMHW coefficients

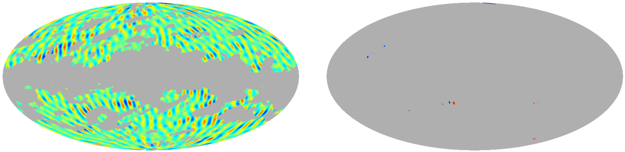

(b) SMW coefficients

Figure: Spherical wavelet coefficient maps (left) and thresholded maps (right)

Dark energy

- Universe consists of ordinary baryonic matter, cold dark matter and dark energy.
- Dark energy represents energy density of empty space. Modelled by a cosmological fluid with negative pressure acting as a repulsive force.
- Evidence for dark energy provided by observations of CMB, supernovae and large scale structure of Universe.

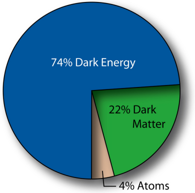

Credit: WMAP Science Team

- However, a consistent model in the framework of particle physics lacking. Indeed, attempts to predict a cosmological constant obtain a value that is too large by a factor of $\sim 10^{120}$.
- Dark energy dominates our Universe but yet we know very little about its nature and origin.
- Verification of dark energy by independent physical methods of considerable interest.
- Independent methods may also prove more sensitive probes of properties of dark energy.

Dark energy

- Universe consists of ordinary baryonic matter, cold dark matter and dark energy.
- Dark energy represents energy density of empty space. Modelled by a cosmological fluid with negative pressure acting as a repulsive force.
- Evidence for dark energy provided by observations of CMB, supernovae and large scale structure of Universe.

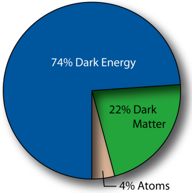

Credit: WMAP Science Team

- However, a consistent model in the framework of particle physics lacking. Indeed, attempts to predict a cosmological constant obtain a value that is too large by a factor of $\sim 10^{120}$.
- Dark energy dominates our Universe but yet we know very little about its nature and origin.
- Verification of dark energy by independent physical methods of considerable interest.
- Independent methods may also prove more sensitive probes of properties of dark energy.

Dark energy

- Universe consists of ordinary baryonic matter, cold dark matter and dark energy.
- Dark energy represents energy density of empty space. Modelled by a cosmological fluid with negative pressure acting as a repulsive force.
- Evidence for dark energy provided by observations of CMB, supernovae and large scale structure of Universe.

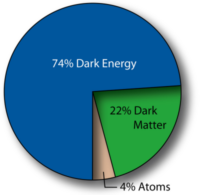

Credit: WMAP Science Team

- However, a consistent model in the framework of particle physics lacking. Indeed, attempts to predict a cosmological constant obtain a value that is too large by a factor of $\sim 10^{120}$.
- Dark energy dominates our Universe but yet we know very little about its nature and origin.
- Verification of dark energy by independent physical methods of considerable interest.
- Independent methods may also prove more sensitive probes of properties of dark energy.

Integrated Sachs-Wolfe (ISW) effect

(ball sim constant movie) (ball sim evolving movie)

Figure: ISW effect analogy

- CMB photons blue (red) shifted when fall into (out of) potential wells.
- Evolution of potential during photon propagation $\longrightarrow$ net change in photon energy.
- Gravitation potentials constant w.r.t. conformal time in matter dominated universe.
- Deviation from matter domination due to curvature or dark energy causes potentials to evolve with time $\longrightarrow$ secondary anisotropy induced in CMB.

Detecting the ISW effect

- WMAP shown universe is (nearly) flat.
- Detection of ISW effect $\Rightarrow$ direct evidence for dark energy.
- Cannot isolate the ISW signal from CMB anisotropies easily.
- Instead, detect by cross-correlating CMB anisotropies with tracers of large scale structure.
  (Crittenden & Turok 1996 [2])
- Wavelets ideal analysis tool to search for correlation induced by ISW effect since signal manifest at different scales and locations.
  (Pioneered by Vielva *et al.* 2005 [7], followed by JDM *et al.* 2006 [5], JDM *et al.* 2007 [6] and others.)
- Compute correlation of WMAP and NVSS radio galaxy survey and compare to Monte Carlo simulations to determine significance of any candidate detections.

Detecting the ISW effect

- WMAP shown universe is (nearly) flat.
- Detection of ISW effect $\Rightarrow$ direct evidence for dark energy.
- Cannot isolate the ISW signal from CMB anisotropies easily.
- Instead, detect by cross-correlating CMB anisotropies with tracers of large scale structure.
  (Crittenden & Turok 1996 [2])
- Wavelets ideal analysis tool to search for correlation induced by ISW effect since signal manifest at different scales and locations.
  (Pioneered by Vielva *et al.* 2005 [7], followed by JDM *et al.* 2006 [5], JDM *et al.* 2007 [6] and others.)
- Compute correlation of WMAP and NVSS radio galaxy survey and compare to Monte Carlo simulations to determine significance of any candidate detections.

Detecting the ISW effect

- WMAP shown universe is (nearly) flat.
- Detection of ISW effect $\Rightarrow$ direct evidence for dark energy.
- Cannot isolate the ISW signal from CMB anisotropies easily.
- Instead, detect by cross-correlating CMB anisotropies with tracers of large scale structure.
  (Crittenden & Turok 1996 [2])
- Wavelets ideal analysis tool to search for correlation induced by ISW effect since signal manifest at different scales and locations.
  (Pioneered by Vielva *et al.* 2005 [7], followed by JDM *et al.* 2006 [5], JDM *et al.* 2007 [6] and others.)
- Compute correlation of WMAP and NVSS radio galaxy survey and compare to Monte Carlo simulations to determine significance of any candidate detections.

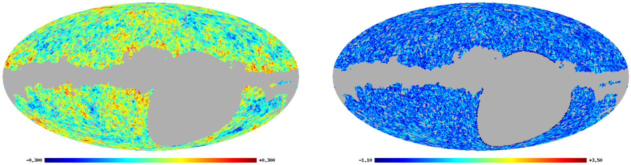

(a) WMAP (b) NVSS

Figure: WMAP and NVSS maps after application of the joint mask

Detection of the ISW effect with wavelets

- Significant correlation detected between the WMAP and NVSS data.
- Foreground contamination and instrumental systematics ruled out as source of the correlation
  $\Rightarrow$ correlation due to ISW effect.
- Direct observational evidence for dark energy.

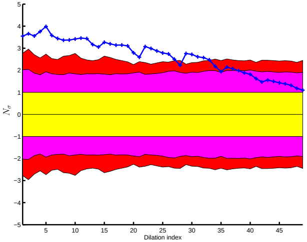

Figure: Wavelet correlation

Detection of the ISW effect with wavelets

- Significant correlation detected between the WMAP and NVSS data.
- Foreground contamination and instrumental systematics ruled out as source of the correlation $\Rightarrow$ correlation due to ISW effect.
- Direct observational evidence for dark energy.

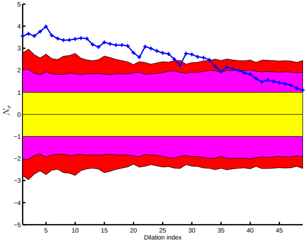

Figure: Wavelet correlation

Constraining dark energy with wavelets

- Possible to use positive detection of the ISW effect to constrain parameters of cosmological models that describe dark energy:
  - Proportional energy density Ω_Λ.
  - Equation of state parameter w relating pressure and density of cosmological fluid that models dark energy, *i.e.* $p = w\rho$.
- Parameter estimates of $\Omega_\Lambda = 0.63^{+0.18}_{-0.17}$ and $w = -0.77^{+0.35}_{-0.36}$ computed from the mean of the marginalised distributions (consistent with other analysis techniques and data sets).

Constraining dark energy with wavelets

- Possible to use positive detection of the ISW effect to constrain parameters of cosmological models that describe dark energy:
  - Proportional energy density Ω_Λ.
  - Equation of state parameter w relating pressure and density of cosmological fluid that models dark energy, *i.e.* $p = w\rho$.
- Parameter estimates of $\Omega_\Lambda = 0.63^{+0.18}_{-0.17}$ and $w = -0.77^{+0.35}_{-0.36}$ computed from the mean of the marginalised distributions (consistent with other analysis techniques and data sets).

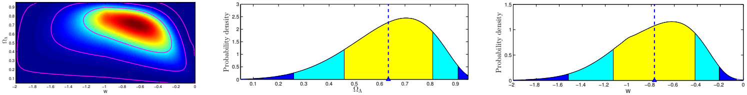

(a) Full likelihood surface (b) Marginalised distribution for Ω_Λ (c) Marginalised distribution for w

Figure: Dark energy likelihoods

Outline

Multiresolution analysis on the sphere

- Define multiresolution analysis on the sphere in an analogous manner to Euclidean framework.
- Define approximation spaces on the sphere $V_j \subset \mathrm{L}^2(\mathbb{S}^2)$
- Construct the nested hierarchy of approximation spaces

$$V_1 \subset V_2 \subset \cdots \subset V_J \subset \mathrm{L}^2(\mathbb{S}^2) \,,$$

where coarser (finer) approximation spaces correspond to a lower (higher) resolution level j.

- For each space V_j we define a basis with basis elements given by the *scaling functions* $\varphi_{j,k} \in V_j$, where the k index corresponds to a translation on the sphere.
- Define detail space W_j to be the orthogonal complement of V_j in V_{j+1}, *i.e.* $V_{j+1} = V_j \oplus W_j$.
- For each space W_j we define a basis with basis elements given by the *wavelets* $\psi_{j,k} \in W_j$.
- Expanding the hierarchy of approximation spaces:

$$V_J = V_1 \oplus \bigoplus_{j=1}^{J-1} W_j \,.$$

Multiresolution analysis on the sphere

- Define multiresolution analysis on the sphere in an analogous manner to Euclidean framework.
- Define approximation spaces on the sphere $V_j \subset \mathrm{L}^2(\mathbb{S}^2)$
- Construct the nested hierarchy of approximation spaces

$$V_1 \subset V_2 \subset \cdots \subset V_J \subset \mathrm{L}^2(\mathbb{S}^2) \; ,$$

where coarser (finer) approximation spaces correspond to a lower (higher) resolution level j.

- For each space V_j we define a basis with basis elements given by the *scaling functions* $\varphi_{j,k} \in V_j$, where the k index corresponds to a translation on the sphere.
- Define detail space W_j to be the orthogonal complement of V_j in V_{j+1}, *i.e.* $V_{j+1} = V_j \oplus W_j$.
- For each space W_j we define a basis with basis elements given by the *wavelets* $\psi_{j,k} \in W_j$.
- Expanding the hierarchy of approximation spaces:

$$V_J = V_1 \oplus \bigoplus_{j=1}^{J-1} W_j \; .$$

Multiresolution analysis on the sphere

- Define multiresolution analysis on the sphere in an analogous manner to Euclidean framework.
- Define approximation spaces on the sphere $V_j \subset \mathrm{L}^2(\mathbb{S}^2)$
- Construct the nested hierarchy of approximation spaces

$$V_1 \subset V_2 \subset \cdots \subset V_J \subset \mathrm{L}^2(\mathbb{S}^2) \, ,$$

where coarser (finer) approximation spaces correspond to a lower (higher) resolution level j.

- For each space V_j we define a basis with basis elements given by the *scaling functions* $\varphi_{j,k} \in V_j$, where the k index corresponds to a translation on the sphere.
- Define detail space W_j to be the orthogonal complement of V_j in V_{j+1}, *i.e.* $V_{j+1} = V_j \oplus W_j$.
- For each space W_j we define a basis with basis elements given by the *wavelets* $\psi_{j,k} \in W_j$.
- Expanding the hierarchy of approximation spaces:

$$V_J = V_1 \oplus \bigoplus_{j=1}^{J-1} W_j \, .$$

Hierarchical pixelisation of the sphere

- Relate generic multiresolution decomposition to HEALPix hierarchical pixelisation of the sphere [3].

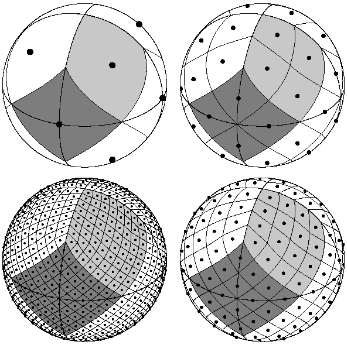

Credit: Krzysztof Gorski

Haar wavelets on the sphere

- Let V_j correspond to a `HEALPix` pixelised sphere with resolution parameter $N_{\text{side}} = 2^{j-1}$.
- Define the scaling function $\varphi_{j,k}$ at level j to be constant for pixel k and zero elsewhere:

$$\varphi_{j,k}(\omega) \equiv \begin{cases} 1/\sqrt{A_j} & \omega \in P_{j,k} \\ 0 & \text{elsewhere} . \end{cases}$$

- Orthonormal basis for the wavelet space W_j given by the following wavelets:

$$\psi^0_{j,k}(\omega) \equiv \left[\varphi_{j+1,k_0}(\omega) - \varphi_{j+1,k_1}(\omega) + \varphi_{j+1,k_2}(\omega) - \varphi_{j+1,k_3}(\omega)\right]/2 ;$$
$$\psi^1_{j,k}(\omega) \equiv \left[\varphi_{j+1,k_0}(\omega) + \varphi_{j+1,k_1}(\omega) - \varphi_{j+1,k_2}(\omega) - \varphi_{j+1,k_3}(\omega)\right]/2 ;$$
$$\psi^2_{j,k}(\omega) \equiv \left[\varphi_{j+1,k_0}(\omega) - \varphi_{j+1,k_1}(\omega) - \varphi_{j+1,k_2}(\omega) + \varphi_{j+1,k_3}(\omega)\right]/2 .$$

Haar wavelets on the sphere

- Let V_j correspond to a `HEALPix` pixelised sphere with resolution parameter $N_{\rm side} = 2^{j-1}$.
- Define the scaling function $\varphi_{j,k}$ at level j to be constant for pixel k and zero elsewhere:

$$\varphi_{j,k}(\omega) \equiv \begin{cases} 1/\sqrt{A_j} & \omega \in P_{j,k} \\ 0 & \text{elsewhere} . \end{cases}$$

- Orthonormal basis for the wavelet space W_j given by the following wavelets:

$$\psi^0_{j,k}(\omega) \equiv \left[\varphi_{j+1,k_0}(\omega) - \varphi_{j+1,k_1}(\omega) + \varphi_{j+1,k_2}(\omega) - \varphi_{j+1,k_3}(\omega)\right]/2 ;$$
$$\psi^1_{j,k}(\omega) \equiv \left[\varphi_{j+1,k_0}(\omega) + \varphi_{j+1,k_1}(\omega) - \varphi_{j+1,k_2}(\omega) - \varphi_{j+1,k_3}(\omega)\right]/2 ;$$
$$\psi^2_{j,k}(\omega) \equiv \left[\varphi_{j+1,k_0}(\omega) - \varphi_{j+1,k_1}(\omega) - \varphi_{j+1,k_2}(\omega) + \varphi_{j+1,k_3}(\omega)\right]/2 .$$

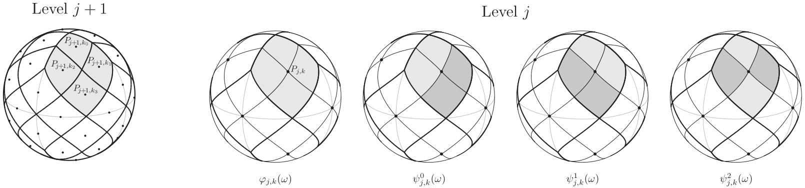

Figure: Haar scaling function $\varphi_{j,k}(\omega)$ and wavelets $\psi^m_{j,k}(\omega)$

Haar wavelets on the sphere

- Multiresolution decomposition of a function defined on a `HEALPix` data-sphere at resolution J, *i.e.* $f_J \in V_J$ proceeds as follows.
- Approximation coefficients at the coarser level j are given by the projection of f_{j+1} onto the scaling functions $\varphi_{j,k}$:

$$\lambda_{j,k} = \int_{\mathbb{S}^2} f_{j+1}(\omega)\, \varphi_{j,k}(\omega)\ \mathrm{d}\Omega\ .$$

- Detail coefficients at level j are given by the projection of f_{j+1} onto the wavelets $\psi^m_{j,k}$:

$$\gamma^m_{j,k} = \int_{\mathbb{S}^2} f_{j+1}(\omega)\, \psi^m_{j,k}(\omega)\ \mathrm{d}\Omega\ .$$

- The function $f_J \in V_J$ may then be synthesised from its approximation and detail coefficients:

$$f_J(\omega) = \sum_{k=0}^{N_{J_0}-1} \lambda_{J_0 k} \varphi_{J_0 k}(\omega) + \sum_{j=J_0}^{J-1} \sum_{k=0}^{N_j-1} \sum_{m=0}^{2} \gamma^m_{j,k} \psi^m_{j,k}(\omega)\ .$$

Haar wavelets on the sphere

- Multiresolution decomposition of a function defined on a HEALPix data-sphere at resolution J, *i.e.* $f_J \in V_J$ proceeds as follows.

- Approximation coefficients at the coarser level j are given by the projection of f_{j+1} onto the scaling functions $\varphi_{j,k}$:

$$\lambda_{j,k} = \int_{\mathbb{S}^2} f_{j+1}(\omega)\ \varphi_{j,k}(\omega)\ \mathrm{d}\Omega\ .$$

- Detail coefficients at level j are given by the projection of f_{j+1} onto the wavelets $\psi^m_{j,k}$:

$$\gamma^m_{j,k} = \int_{\mathbb{S}^2} f_{j+1}(\omega)\ \psi^m_{j,k}(\omega)\ \mathrm{d}\Omega\ .$$

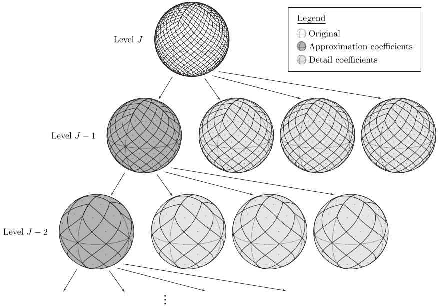

Figure: Haar multiresolution decomposition

- The function $f_J \in V_J$ may then be synthesised from its approximation and detail coefficients:

$$f_J(\omega) = \sum_{k=0}^{N_{J_0}-1} \lambda_{J_0 k}\varphi_{J_0 k}(\omega) + \sum_{j=J_0}^{J-1}\sum_{k=0}^{N_j-1}\sum_{m=0}^{2} \gamma^m_{j,k}\psi^m_{j,k}(\omega)\ .$$

Haar wavelets on the sphere

- Multiresolution decomposition of a function defined on a HEALPix data-sphere at resolution J, *i.e.* $f_J \in V_J$ proceeds as follows.
- Approximation coefficients at the coarser level j are given by the projection of f_{j+1} onto the scaling functions $\varphi_{j,k}$:

$$\lambda_{j,k} = \int_{\mathbb{S}^2} f_{j+1}(\omega)\ \varphi_{j,k}(\omega)\ \mathrm{d}\Omega\ .$$

- Detail coefficients at level j are given by the projection of f_{j+1} onto the wavelets $\psi^m_{j,k}$:

$$\gamma^m_{j,k} = \int_{\mathbb{S}^2} f_{j+1}(\omega)\ \psi^m_{j,k}(\omega)\ \mathrm{d}\Omega\ .$$

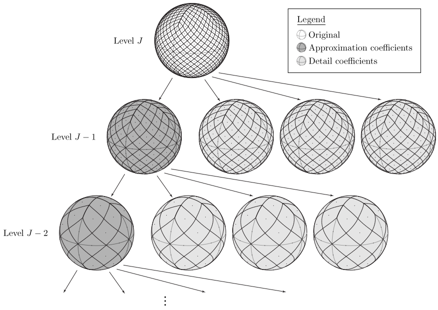

Figure: Haar multiresolution decomposition

- The function $f_J \in V_J$ may then be synthesised from its approximation and detail coefficients:

$$f_J(\omega) = \sum_{k=0}^{N_{J_0}-1} \lambda_{J_0 k}\varphi_{J_0 k}(\omega) + \sum_{j=J_0}^{J-1}\sum_{k=0}^{N_j-1}\sum_{m=0}^{2} \gamma^m_{j,k}\psi^m_{j,k}(\omega)\ .$$

Compression of data on the sphere

- Current and forthcoming observations of the CMB of considerable size.
- Haar wavelet transform to compress energy content.

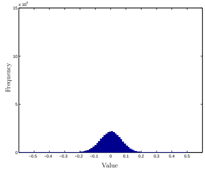

(a) Original data

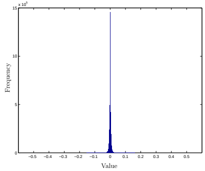

(b) Wavelet coefficients

Figure: Histograms

Compression of data on the sphere

- Current and forthcoming observations of the CMB of considerable size.
- Haar wavelet transform to compress energy content.

Lossless compression algorithm

1. Haar wavelet transform on sphere
2. Quantise detail coefficients to numerical precision (precision parameter p)
3. Huffman encoding

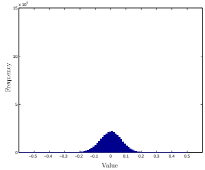

(a) Original data

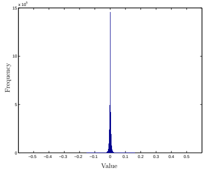

(b) Wavelet coefficients

Figure: Histograms

Compression of data on the sphere

- Current and forthcoming observations of the CMB of considerable size.
- Haar wavelet transform to compress energy content.

Lossless compression algorithm

1. Haar wavelet transform on sphere
2. Quantise detail coefficients to numerical precision (precision parameter p)
3. Huffman encoding

Lossy compression algorithm

1. Haar wavelet transform on sphere
2. Thresholding
3. Quantise detail coefficients to numerical precision
4. Run-length encoding (RLE)
5. Huffman encoding

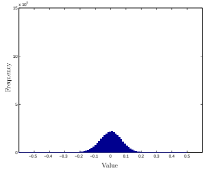

(a) Original data

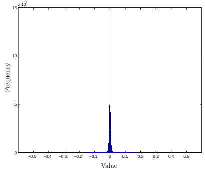

(b) Wavelet coefficients

Figure: Histograms

Compression of CMB data

- Lossless to a user specified numerical precision only.

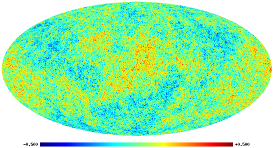

(a) Original for $N_{\text{side}} = 512$ (13MB)

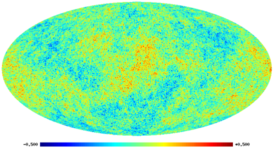

(b) Compressed for $N_{\text{side}} = 512$ (2.5MB)

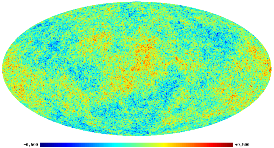

(c) Original for $N_{\text{side}} = 1024$ (50MB)

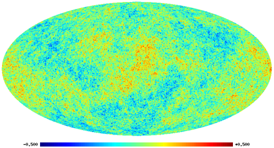

(d) Compressed for $N_{\text{side}} = 1024$ (9.1MB)

Figure: Lossless compression of simulated Gaussian CMB data

Lossy compression applications

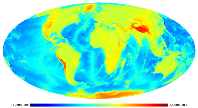

(a) Earth: original (13MB)

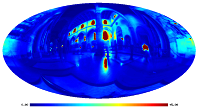

(b) Galileo: original (3.2MB)

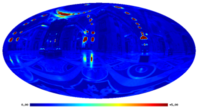

(c) St Peter's: original (3.2MB)

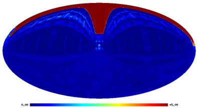

(d) Uffizi: original (3.2MB)

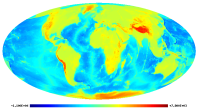

(e) Earth: lossless (1.4MB)

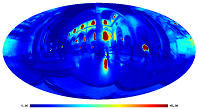

(f) Galileo: lossless (0.21MB)

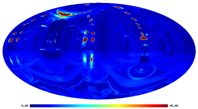

(g) St Peter's: lossless (0.20MB)

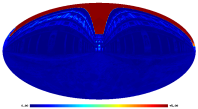

(h) Uffizi: lossless (0.19MB)

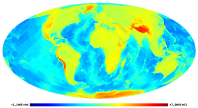

(i) Earth: lossy (0.33MB)

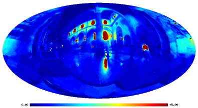

(j) Galileo: lossy (0.07MB)

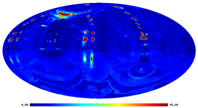

(k) St Peter's: lossy (0.08MB)

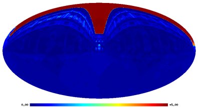

(l) Uffizi: lossy (0.10MB)

Figure: Compressed data for lossy compression applications

Outline

Summary

- Wavelet analyses have many applications in physics and allow one to probe physical processes manifest on different scales and locations.
- Data are often defined on manifolds other than Euclidean space, such as the sphere, which motivate novel wavelet transforms.
- Observations of the CMB are inherently made on the celestial sphere due to the original singularity and subsequent expansion of the Universe.
- Analyses of the CMB have lead to a cosmological concordance model, however many exotic details still to be resolved.
- Wavelet analyses of the CMB have been used to detect non-Gaussianity in the CMB, suggesting deviations from standard cosmological model, and to detect and constrain dark energy.
- Continuous wavelet analyses on the sphere allow one to probe physical processes but discrete frameworks required to reconstruct signals on the sphere
  $\longrightarrow$ opens door to new class of physical problem.

- Student projects (see http://lts2www.epfl.ch/Main/StudentProjects):
  - Denoising and deconvolution on the sphere with application to cosmology and computer vision.
  - Compressed sensing techniques for radio interferometric imaging on wide fields of view.

Summary

- Wavelet analyses have many applications in physics and allow one to probe physical processes manifest on different scales and locations.
- Data are often defined on manifolds other than Euclidean space, such as the sphere, which motivate novel wavelet transforms.
- Observations of the CMB are inherently made on the celestial sphere due to the original singularity and subsequent expansion of the Universe.
- Analyses of the CMB have lead to a cosmological concordance model, however many exotic details still to be resolved.
- Wavelet analyses of the CMB have been used to detect non-Gaussianity in the CMB, suggesting deviations from standard cosmological model, and to detect and constrain dark energy.
- Continuous wavelet analyses on the sphere allow one to probe physical processes but discrete frameworks required to reconstruct signals on the sphere
  $\longrightarrow$ opens door to new class of physical problem.
- Student projects (see http://lts2www.epfl.ch/Main/StudentProjects):
  - Denoising and deconvolution on the sphere with application to cosmology and computer vision.
  - Compressed sensing techniques for radio interferometric imaging on wide fields of view.

Summary

- Wavelet analyses have many applications in physics and allow one to probe physical processes manifest on different scales and locations.
- Data are often defined on manifolds other than Euclidean space, such as the sphere, which motivate novel wavelet transforms.
- Observations of the CMB are inherently made on the celestial sphere due to the original singularity and subsequent expansion of the Universe.
- Analyses of the CMB have lead to a cosmological concordance model, however many exotic details still to be resolved.
- Wavelet analyses of the CMB have been used to detect non-Gaussianity in the CMB, suggesting deviations from standard cosmological model, and to detect and constrain dark energy.
- Continuous wavelet analyses on the sphere allow one to probe physical processes but discrete frameworks required to reconstruct signals on the sphere
$\longrightarrow$ opens door to new class of physical problem.
- Student projects (see `http://lts2www.epfl.ch/Main/StudentProjects`):
    - Denoising and deconvolution on the sphere with application to cosmology and computer vision.
    - Compressed sensing techniques for radio interferometric imaging on wide fields of view.

Summary

- Wavelet analyses have many applications in physics and allow one to probe physical processes manifest on different scales and locations.
- Data are often defined on manifolds other than Euclidean space, such as the sphere, which motivate novel wavelet transforms.
- Observations of the CMB are inherently made on the celestial sphere due to the original singularity and subsequent expansion of the Universe.
- Analyses of the CMB have lead to a cosmological concordance model, however many exotic details still to be resolved.
- Wavelet analyses of the CMB have been used to detect non-Gaussianity in the CMB, suggesting deviations from standard cosmological model, and to detect and constrain dark energy.
- Continuous wavelet analyses on the sphere allow one to probe physical processes but discrete frameworks required to reconstruct signals on the sphere
  $\longrightarrow$ opens door to new class of physical problem.
- Student projects (see `http://lts2www.epfl.ch/Main/StudentProjects`):
  - Denoising and deconvolution on the sphere with application to cosmology and computer vision.
  - Compressed sensing techniques for radio interferometric imaging on wide fields of view.

References I

[1] J.-P. Antoine and P. Vandergheynst.
Wavelets on the n-sphere and related manifolds.
J. Math. Phys., 39(8):3987–4008, 1998.

[2] Robert G. Crittenden and Neil Turok.
Looking for Λ with the Rees-Sciama effect.
Phys. Rev. Lett., 76:575–578, 1996.

[3] K. M. Górski, E. Hivon, A. J. Banday, B. D. Wandelt, F. K. Hansen, M. Reinecke, and M. Bartelmann.
Healpix – a framework for high resolution discretization and fast analysis of data distributed on the sphere.
Astrophys. J., 622:759–771, 2005.

[4] J. D. McEwen, M. P. Hobson, D. J. Mortlock, and A. N. Lasenby.
Fast directional continuous spherical wavelet transform algorithms.
IEEE Trans. Sig. Proc., 55(2):520–529, 2007.

[5] J. D. McEwen, P. Vielva, M. P. Hobson, E. Martínez-González, and A. N. Lasenby.
Detection of the ISW effect and corresponding dark energy constraints made with directional spherical wavelets.
Mon. Not. Roy. Astron. Soc., 373:1211–1226, 2007.

References II

[6] J. D. McEwen, Y. Wiaux, M. P. Hobson, P. Vandergheynst, and A. N. Lasenby.
Probing dark energy with steerable wavelets through correlation of WMAP and NVSS local morphological measures.
ArXiv, 2007.

[7] P. Vielva, E. Martínez-González, and M. Tucci.
Cross-correlation of the cosmic microwave background and radio galaxies in real, harmonic and wavelet spaces: detection of the integrated Sachs-Wolfe effect and dark energy constraints.
Mon. Not. Roy. Astron. Soc., 365:891–901, 2006.

[8] Y. Wiaux, L. Jacques, and P. Vandergheynst.
Correspondence principle between spherical and Euclidean wavelets.
Astrophys. J., 632:15–28, 2005.

[9] Y. Wiaux, J. D. McEwen, and P. Vielva.
Complex data processing: fast wavelet analysis on the sphere.
J. Fourier Anal. and Appl., invited contribution, in press, 2007.

[10] Yves Wiaux, L. Jacques, P. Vielva, and P. Vandergheynst.
Fast directional correlation on the sphere with steerable filters.
Astrophys. J., 652:820–832, 2006.